Dynamical Seasonal Prediction of Typhoones with the New Coupled Model (JMA/MRI-CGCM)

Yuhei Takaya[1], Tamaki Yasuda[2], Hirotaka Kamahori[1], Tomoaki Ose[2]
[1]Climate Prediction Division, Japan Meteorological Agency, Japan
[2]Meteorological Research Institute, Japan Meteorological Agency, Japan
Correspondence: ytakaya@met.kishou.go.jp

INTRODUCTION

The western North Pacific is the most active region of tropical storms all over the world. East Asian countries suffer from massive socio-economic damage caused by typhoons. Therefore, the skillful seasonal forecast of typhoons is anticipated to mitigate these economic losses. To meet this demand, several national meteorological services and research groups currently issue the seasonal forecast of tropical cyclones (TCs) (Camargo et al. 2007). Furthermore, the skillful seasonal forecast of TCs activity was demonstrated with coupled models (Vitart and Stockdale 2001; Vitart 2006; Vitart et al. 2007). Recently, the Japan Meteorological Agency (JMA) and the Meteorological Research Institute (MRI) have developed a new atmosphere-ocean coupled model (JMA/MRI-CGCM). In this study, we evaluate the performance of the typhoon seasonal forecast with the new model. Additionally, the TC predictability associated with ENSO and the monsoon trough is illustrated with our forecast results.

EXPERIMENTAL SETTING and ANALYSIS PROCEDURE

1) Forecast system

The forecast system used in this study is the same as the next version of the JMA ENSO forecast system that will be operated from March 2008. The forecast system is composed of the coupled model (JMA/MRI-CGCM) and an ocean data assimilation system (MOVE/MRI.COM-G; Usui et al. 2006). The atmospheric component of the coupled model has T_L95 spectral resolution (~180 km) and 40 vertical levels. An ocean model resolution is 1.0° (longitude)×0.3-1.0° (latitude) with 50 vertical levels (24 levels in the upper 200 m). Atmospheric initial conditions are given from JRA-25 reanalysis (Onogi et al. 2007) and its real time analysis JCDAS. The ocean data assimilation system is driven with atmospheric forcing of JRA-25 and JCDAS, so we can get homogeneous and consistent hindcast results with JRA-25 and JCDAS. These results are important for appropriate calibrations of the real-time forecast.

2) Experimental setting and reference data

The hindcast experiment was conducted following the experimental design of the World Climate Research Program (WCRP) Task Force on Seasonal Prediction (TFSP) experiment. A 10-member ensemble forecast was carried out for 28 years (1979-2006). The forecast runs were initiated from the end of April. Initial conditions were produced by the Lagged Average Forecast (LAF) method. A forecast period is the western North Pacific typhoon season (June-October). Daily data at 00UTC were used for detecting TCs.

Best track data distributed by the RSMC Tokyo Typhoon Center (RSMC Tokyo) and the Joint Tropical Cyclone Warning Center (JTWC) are used as the reference data. The JRA-25 and JCDAS data with the resolution of 1.25° are used to verify skill of the TC forecast. The CPC Merged Analysis of Precipitation (CMAP; Xie and Arkin 1997) data is used for reference data of precipitation.

3) An algorithm for detecting and tracking TCs

In this study, TCs which have maximum wind speed of larger than 17 m s^{-1} (34 kt) were analyzed. We used an objective algorithm based on sea level pressure (SLP), relative vorticity at 850 hPa, middle to upper tropospheric thickness, and wind speed at 850 hPa and 200 hPa. We selected the following conditions for detection of TCs in the model:

[1] Grid points over the ocean between the equator and 40°N with a local minimum of sea level pressure within 7×7 grid points are selected for the possible center positions of TCs.

Following three conditions [2]-[4] must be satisfied on at least one point within inner 9 points of 3×3 points near a TC center location.

[2] The relative vorticity larger than a threshold. The thresholds depend on the resolution and the TC feature in the analysis and the model. The thresholds for JRA-25 and the model are set to 7.5×10^{-5} s^{-1} and 4.5×10^{-5} s^{-1} respectively.

[3] TCs have the warm core structure defined by 500-200 hPa thickness anomaly from an average of surrounding 2 grid rows. (The anomaly thresholds for JRA-25 and the model are set to 10 gpm and 5 gpm respectively.)

[4] TCs have the wind structure that the wind speed at 850 hPa is larger than 200 hPa. We added this condition to exclude extratropical cyclones which have a baroclinic vertical structure.

[5] The conditions described above ([1]-[4]) must continue at least 2 days for disturbances to be counted as TCs.

For tracking TCs, we search the previous TCs within a 15°×15° box. TCs continue more than 2 days are exempted from conditions [3] and [4], and the vorticity criterion is related to 70% of the original threshold.

RESULTS

1) Validation of the algorithm for TC detection

The TC detection algorithm was validated with JRA-25 data. It was pointed out that TCs in JRA-25 have more coherent structure and more rapid intensification in their early stage than ERA-40 (Bengtsson et al. 2007). Therefore, we think JRA-25 data are proper for testing the TC detection algorithm. Figure 1 shows the interannual variability of the number of TC formation. The number of TC formation detected with our algorithm from JRA-25 was consistent to the RSMC Tokyo best track data except for some years. The correlation between the RSMC Tokyo best track and JRA-25 data was 0.46. Excluding 3 outliers (1988, 1989, 1990), the correlation increased to 0.65. The number of TC days, which refers to the number of days TC existed, in JRA-25 was very close to RSMC Tokyo best track. The correlation was 0.93. For the location of TC formation, the mean latitude and longitude of TC formation in JRA-25 were roughly matched RSMC Tokyo best track. The correlations of mean longitude and latitude between JRA-25 and RSMC Tokyo best track are 0.70 and 0.80 respectively. These results demonstrate that our algorithm is effective for detecting TCs.

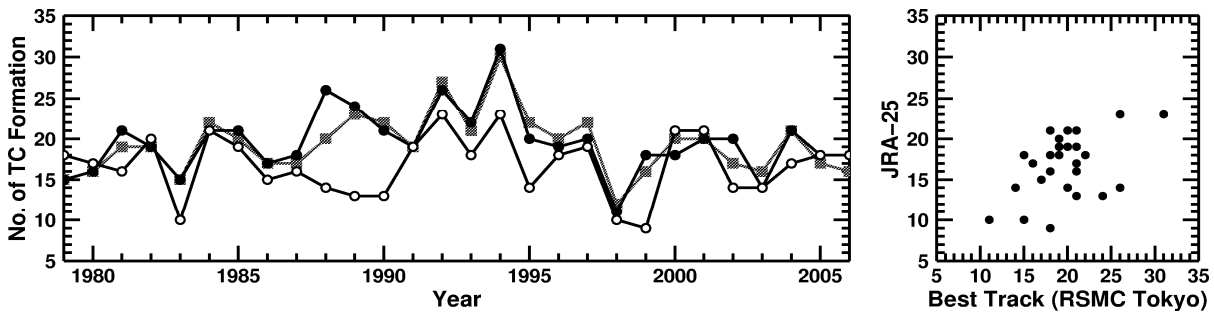

Figure 1 (left) The number of TC formation in the western North Pacific. Open circles: ensemble forecast mean, closed circles: the RSMC Tokyo best track data, closed squares: and the JTWC best track data. (right) The scatter plot of the number of TC formation.

2) Verification results of the forecast

Applying the TC detection algorithm to the forecast data, we assessed the performance of TC forecast with the new coupled model. Figure 2 shows the forecast result of the number of TC formation in the western North Pacific. The correlation is 0.23 for the period of 1979-2006. Verifying between the period of 1995-2006, the better score of 0.63 was achieved.

Next, we verified the mean location of TC formation. The mean location of TC formation in the western North Pacific is associated with the ENSO variability (e.g., Lander 1994; Chia and Ropelewski 2002; Wang and Chan 2002). Vitart and Stockdale (2001) reported that the mean location of TC formation in the western north Pacific in 1997 and 1998 are well predicted with the ECMWF forecast system. Figure 3 shows the interannual variability of the mean latitude of TC formation. The model predicts well the mean latitude of TC formation. The correlation is 0.68. Figure 4 shows forecast results of the mean longitude of TC formation. Although the model has westward bias, there is an agreement in some years. The correlation is 0.53. The westward bias caused by the excess TC formation in South China Sea in the model (not shown).

The new model shows some skill for the mean location of TC formation. This predictability result from the relationship with ENSO. Wand and Chan (2002) found out that the number of TC formation in the southeastern (SE) part (eq.-17.5°N, 140°E-180°) and northwestern (NW) part (17.5°-30°N, 120°-140°E) are strongly associated with ENSO variability. So we verified the number of TC formation in the SE part. The number of TC formation in the SE part is well predicted, and the correlation is 0.72. We also examined results of the NW part, but we couldn't find meaningful skill in this region. This is because environmental conditions were not predicted enough.

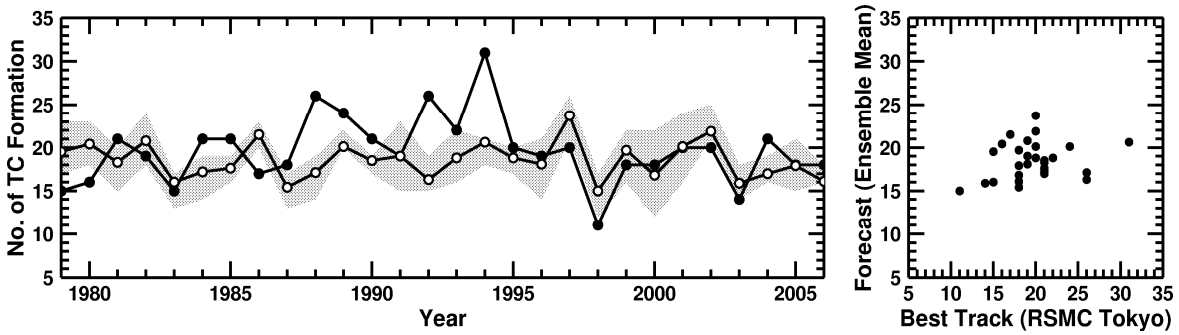

Figure 2 (left) The forecast result of the number of TC formation in the western North Pacific. Closed circles: the RSMC Tokyo best track data, open circles: ensemble mean, shading: the 60% range of the ensemble forecast. (right) The Scatter plot of the number of TC formation.

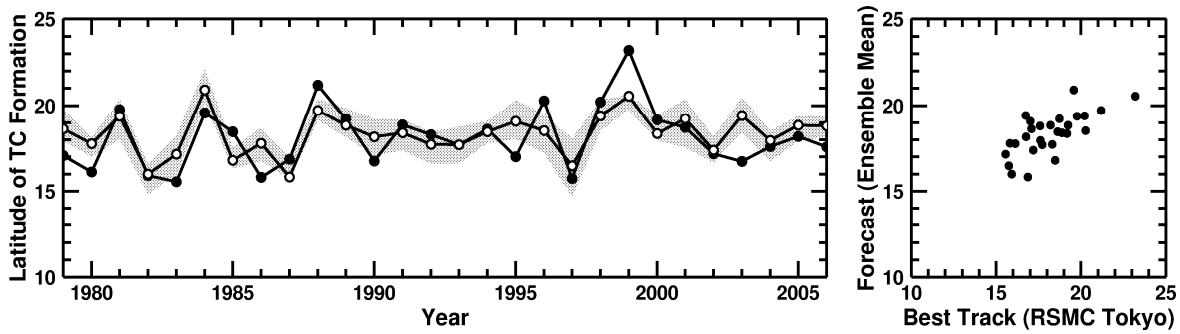

Figure 3 Same as Figure 2 but for the mean latitude of TC formation in the western North Pacific.

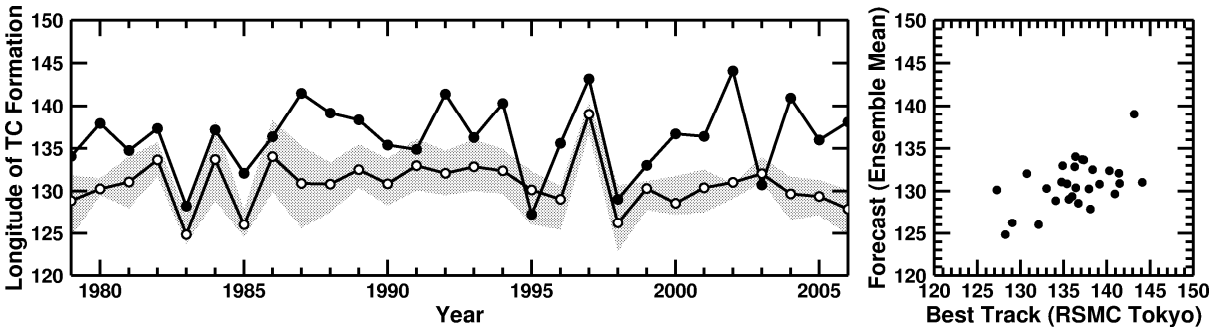

Figure 4 Same as Figure 3 but for the mean longitude of TC formation in the western North Pacific.

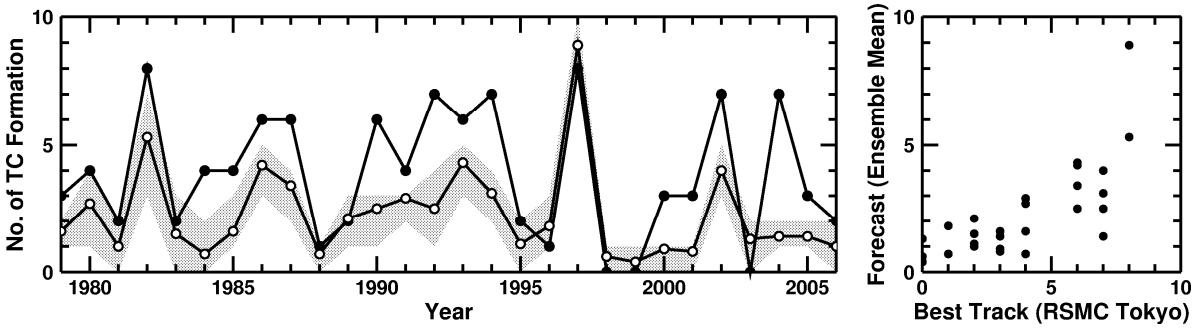

Figure 5 Same as Figure 2 but for the southeastern part of the western North Pacific (Eq.-17.5°N, 140°E-180°).

3) Relationship between TC activity and the monsoon trough

To elucidate the origin of the good skill of TC activity in the southeast part, we investigated the environmental conditions related to TC formation. Particularly we focus on the relationship between TC activity and the monsoon trough. More than 75% of TCs are generated in the monsoon trough region (Ritchie and Holland 1999). The eastward extension and westward retreat of the monsoon trough are associated with the location of TC formation (Chen and Weng 1998).

Figure 6 shows 850-hPa streamline and precipitation anomalies during the typhoon season of the 1997 El Niño year. Analysis shows enhanced and suppressed convection in the SE part and around Philippines respectively. The monsoon trough extends from the north of Philippines to around 5°N, 170°E. The coupled model predicted these features and enhanced TC activity in the SE part. Figure 7 shows the results of the 1998 La Niña year. The westward retreat of the monsoon trough and suppressed convective activity in the SE part are found in the analysis and the forecast result. In other significant El Nino (1982, 1987, 2002) and La Nina (1988, 1999) years, the model predicted well these characteristic conditions (not shown).

As shown in Figure 6 and 7, the model reproduced the conditions related to ENSO such as extension of the monsoon trough and convective activity. So, we conclude the successful forecast of TC activity in the SE part results from the predictability of these ENSO related environmental conditions.

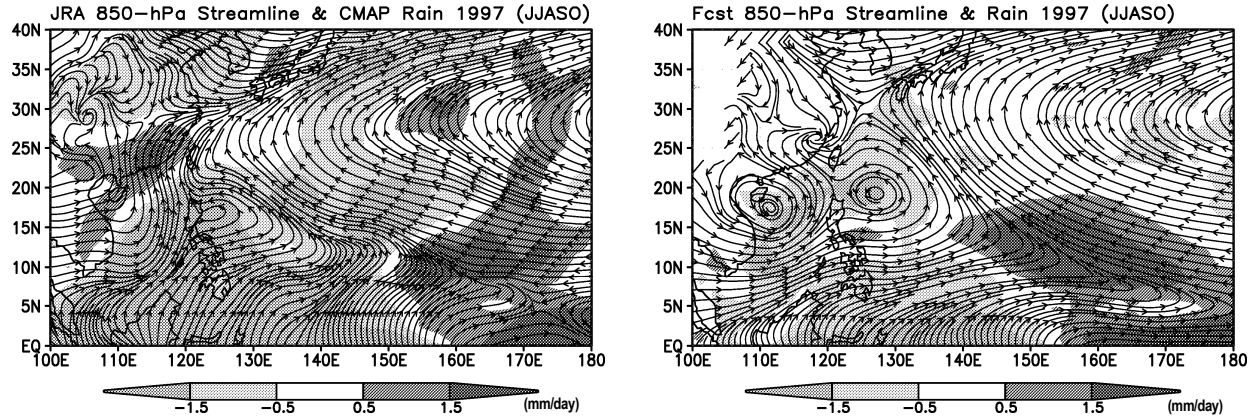

Figure 5 Five-month (JJASO) mean streamline at 850 hPa and precipitation anomalies in 1997. (left) JRA-25 and CMAP data and (right) ensemble forecast.

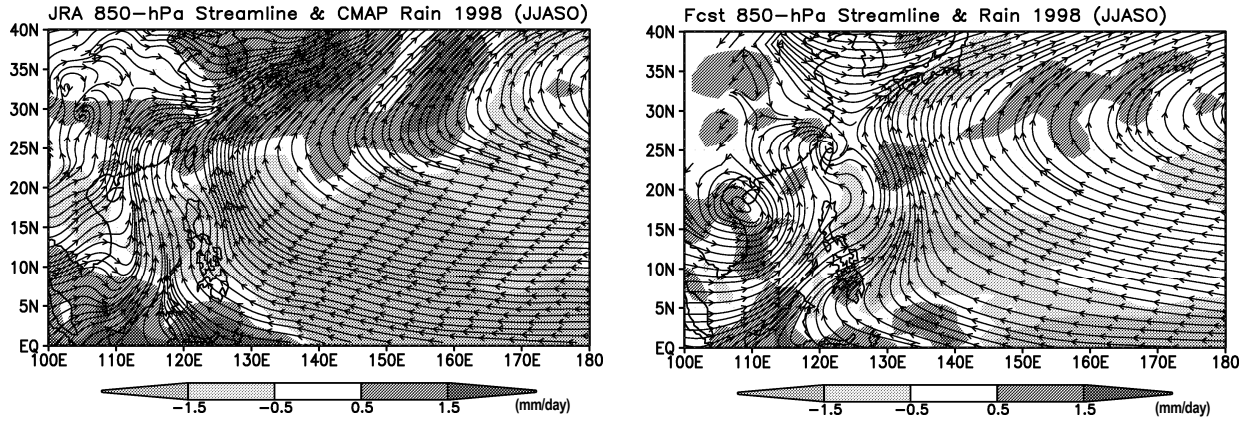

Figure 6 Same as Figure 5 but for 1998.

REFERENCES

Bengtsson, L., K. I. Hodges and M. Esch 2007: Tropical cyclones in a T159 resolution global climate model: comparison with observations and re-analyses. Tellus, **59A**, 396-416.

Camargo, S. J., A. G. Barnston, P. J. Klotzbach and . C. W. Landsea 2007: Seasonal tropical cyclone forecasts. World Meteorological Organization Bulletin, **56** (4), 297-309.

Chen, T.-C. and S.-P. Weng 1998: Interannual Variation of the Summer Synoptic-Scale Disturbance Activity in the Western Tropical Pacific. Mon. Wea. Rev., **126**, 1725-1733.

Chia, H. H. and C. F. Ropelewski 2002: The interannual variability in the genesis location of tropical cyclones in the Northwest Pacific. J. Climate, **15**, 2934-2944.

Lander, M. A. 1994: An exploratory analysis of the relationship between tropical storm formation in the western North Pacific and ENSO. Mon. Wea. Rev., **122**, 636-651.

Onogi, K., J. Tsutsui, H. Koide, M. Sakamoto, S. Kobayashi, H. Hatsushika, T. Matsumoto, N. Yamazaki, H. Kamahori, K. Takahashi, S. Kadokura, K. Wada, K. Kato, R. Oyama, T. Ose, N. Mannoji and R. Taira 2007: The JRA-25 Reanalysis. J. Meteor. Soc. Japan, **85**, 369-432.

Ritchie, E. A. and G. J. Holland 1999: Large-Scale Patterns Associated with Tropical Cyclogenesis in the Western Pacific. Mon. Wea. Rev. **127**, 2027-2043.

Usui, N., S. Ishizaki, Y. Fujii, H. Tsujino, T. Yasuda and M. Kamachi 2006: Meteorological Research Institute

multivariate ocean variational estimation (MOVE) system. Advances in Space Research, **37**, 806-822.
Vitart, F. and T. N. Stockdale 2001: Seasonal forecasting of tropical storms using coupled GCM integrations. Mon. Wea. Rev., **129**, 2521-2537.
Vitart, F. 2006: Seasonal forecasting of tropical storm frequency using a multi-model ensemble. Quart. J. Roy. Meteor. Soc., **132**, 647-666.
Vitart, F., M. R. Huddleston, M. Deque, D. Peake, T. N. Palmer, T. N. Stockdale, M. K. Davey, S. Ineson and A. Weisheimer 2007: Dynamically-based seasonal forecasts of Atlantic tropical storm activity issued in June by EUROSIP. Geophys. Res. Lett., **34**, L16815, doi:10.1029/2007GL030740.
Wang, B. and J. C. L. Chan 2002: How strong ENSO events affect tropical storm activity over the western North Pacific. J. Climate, **15**, 1643-1658.
Xie, P. and P.A. Arkin 1997: Global precipitation: A 17-year monthly analysis based on gauge observations, satellite estimates, and numerical model outputs. Bull. Amer. Meteor. Soc., **78**, 2539 - 2558.